

High-Performance GaAs/AlAs Terahertz Quantum-Cascade Lasers For Spectroscopic Applications

Lutz Schrottke¹, Xiang Lü¹, Benjamin Röben¹, Klaus Biermann¹, Till Hagelschuer¹, Martin Wienold, Heinz-Wilhelm Hübers¹, Mario Hannemann, Jean-Pierre H. van Helden¹, Jürgen Röpcke, and Holger T. Grahn¹

Abstract—We have developed terahertz (THz) quantum-cascade lasers (QCLs) based on GaAs/AlAs heterostructures for application-defined emission frequencies between 3.4 and 5.0 THz. Due to their narrow line width and rather large intrinsic tuning range, these THz QCLs can be used as local oscillators in airborne or satellite-based astronomical instruments or as radiation sources for high-resolution absorption spectroscopy, which is expected to allow for a quantitative determination of the density of atoms and ions in plasma processes. The GaAs/AlAs THz QCLs can be operated in mechanical cryocoolers and even in miniature cryocoolers due to the comparatively high wall-plug efficiency of around 0.2% and typical current densities below 500 A/cm². These lasers emit output powers of more than 1 mW at operating temperatures up to about 70 K, which is sufficient for most of the abovementioned applications.

Index Terms—Quantum-cascade laser (QCLs), terahertz (THz) spectroscopy.

I. INTRODUCTION

THE invention of quantum-cascade lasers (QCLs) about 25 years ago [1] opened the path to a variety of spectroscopic approaches in the mid- to far-infrared spectral region. In particular, QCLs for the terahertz (THz) spectral region [2] allow for high-resolution spectroscopy of molecules, atoms, and ions utilizing rotational or fine-structure transitions. During the

last decade, THz QCLs have been developed for the use as local oscillators in heterodyne receivers for astronomy [3]–[5]. Since 2014, a THz QCL developed at the Paul-Drude-Institut has been employed as the local oscillator on board of Stratospheric Observatory For Infrared Astronomy (SOFIA) for the detection of interstellar atomic oxygen [6]. In atmospheric science, the rotational transition of OH at 3.55 THz and the fine-structure line of atomic oxygen (OI) at 4.75 THz are of particular interest. Both can be measured with QCL-based heterodyne receivers. This approach is, for example, proposed for Link Observations of Climate, the Upper-atmosphere and Space-weather (LOCUS).¹ For fundamental research and industrial applications, high-resolution absorption spectroscopy based on fine-structure transitions in Al, N⁺, and O at 3.36, 3.92, and 4.75 THz, respectively, is expected to allow for the quantitative determination of the atom and ion densities in plasma processes. Furthermore, QCLs emitting in the atmospheric windows around 3.43, 4.32, and 4.92 THz are of interest for applications such as THz spectroscopy under pulsed megagauss magnetic fields at high-magnetic-field facilities, if the THz radiation has to be transmitted through air over a distance of about 10 m into the magnet inside a Faraday cage.

Due to their high emission powers and narrow line widths in continuous-wave (cw) operation, THz QCLs are excellent radiation sources for high-resolution spectroscopy. For such applications, they have to emit radiation at a well-defined frequency, but also have to exhibit an intrinsic tuning range of 5–10 GHz. Such a tuning range is necessary in order to analyze the line shape of an absorption line, e.g., for the quantitative determination of the density of the investigated species. A similar tuning behavior allows for the detection of a possible Doppler shift of radiation received from interstellar objects recorded by heterodyne techniques. For practical use, THz QCLs have to fulfill particular specifications for the intended applications. First of all, the wall-plug efficiency has to be sufficiently high for operation in a mechanical cryocooler or even miniature cryocooler for compactness and to avoid the usage of liquid coolants. We recently demonstrated that THz QCLs based on GaAs/AlAs heterostructures [7] exhibit significantly larger wall-plug efficiencies than similar lasers relying on Al_{0.25}Ga_{0.75}As barriers so that these lasers are preferred for liquid-coolant-free operation.

Manuscript received August 1, 2019; revised October 29, 2019; accepted November 26, 2019. Date of publication December 6, 2019; date of current version March 3, 2020. This work was supported in part by Leibniz-Gemeinschaft under Grant K54/2017 and in part by the European Space Agency through Subcontract D/973/67268909 to ESA Contract 4000125911/18/NL/AF. (Corresponding author: Lutz Schrottke.)

L. Schrottke, X. Lü, B. Röben, K. Biermann, and H. T. Grahn are with the Paul-Drude-Institut für Festkörperelektronik, Leibniz-Institut im Forschungsverbund Berlin e. V., 10117 Berlin, Germany (e-mail: lutz@pdi-berlin.de; lue@pdi-berlin.de; roeben@pdi-berlin.de; biermann@pdi-berlin.de; htgrahn@pdi-berlin.de).

T. Hagelschuer is with German Aerospace Center (DLR), Institute of Optical Sensor Systems, 12489 Berlin, Germany (e-mail: till.hagelschuer@dlr.de).

M. Wienold and H.-W. Hübers are with German Aerospace Center (DLR), Institute of Optical Sensor Systems, 12489 Berlin, Germany, are also with the Humboldt-Universität zu Berlin, Department of Physics, 12489 Berlin, Germany (e-mail: martin.wienold@dlr.de; heinz-wilhelm.huebers@dlr.de).

M. Hannemann, J.-P. H. van Helden, and J. Röpcke are with the Leibniz Institute for Plasma Science and Technology (INP), 17489 Greifswald, Germany (e-mail: hannemann@inp-greifswald.de; jean-pierre.vanhelden@inp-greifswald.de; roepcke@inp-greifswald.de).

Color versions of one or more of the figures in this article are available online at <http://ieeexplore.ieee.org>.

Digital Object Identifier 10.1109/TTHZ.2019.2957456

¹www.locussatellite.com

Second, QCLs are the source of choice for many applications if a cw output power of at least 1 mW is necessary. This output power has to be correlated with a maximum operating temperature. Hence, we define a *practical operating temperature* T_{po} as the temperature at which the QCL exhibits an output power of at least 1 mW emitted in a fundamental Gaussian mode.

For a near-Gaussian beam profile, QCLs with so-called surface plasmon waveguides [2] are used. However, they require designs with rather large gain in order to compensate for the lower mode confinement factor compared to the one for metal-metal waveguides [8]. In particular, for cw operation, lasers with a high gain and a low electrical pumping power, i.e., lasers with a high wall-plug efficiency, are preferred. Here, so-called hybrid designs, in which a bound-to-continuum transition is combined with direct carrier injection or resonant population of injector levels assisted by longitudinal optical phonon emission [9], have proven to be of advantage [5].

In this article, we present THz QCLs based on GaAs/AlAs heterostructures with emission frequencies between 3.4 and 5.0 THz based on the hybrid design, substantially extending the accessible spectral range of lasers based on this materials system, which has been so far reported only for 4.75 THz. Although the growth remains challenging, we have realized lasers from 11 different wafers. Optimized lasers exhibit competitive wall-plug efficiencies and rather high practical operating temperatures in cw operation. Finally, we demonstrate the operation of these THz QCLs in a mechanical cryocooler (Ricor K535) or a miniature cryocooler (AIM SL400).

II. DESIGNS

For the development of the designs, we started from a laser structure operating at 4.75 THz (sample B in [10]), followed by a gradual scaling of the layer structure toward lower or higher frequencies. The QCL structures consist of 78 periods for frequencies smaller than or equal to 3.90 THz and 88 periods for frequencies larger than 3.90 THz using in all cases 8 quantum wells in each period. The corresponding frequencies of the gain maxima are achieved by an appropriate adjustment of the quantum well thicknesses and a corresponding fine-tuning of the thicknesses of some particular barriers. The quantum well, which contains the transition resonant to the energy of the longitudinal optical phonon, is Si doped with a density of up to $2 \times 10^{17} \text{ cm}^{-3}$. Fig. 1(a) and (b) depicts the calculated subband structures using the nominal layer thicknesses of the designs for 4.75 THz and 3.50 THz, respectively, as examples, which demonstrates that the scaling maintains the essential subband structure. Similar designs have been demonstrated by Köhler *et al.* [11] and Scalari *et al.* [12] for the GaAs/Al_{0.15}Ga_{0.85}As materials system with significantly lower doping levels.

In addition to the hybrid character of the design, i.e., the combination of a *bound-to-continuum* laser transition with an efficient carrier extraction from the quasi-miniband and a resonant population of the injector levels utilizing scattering by longitudinal optical phonons, a unique feature of the present design compared to other recent hybrid designs such as discussed by Amanti *et al.* [13] is an undoped *injector* quantum well

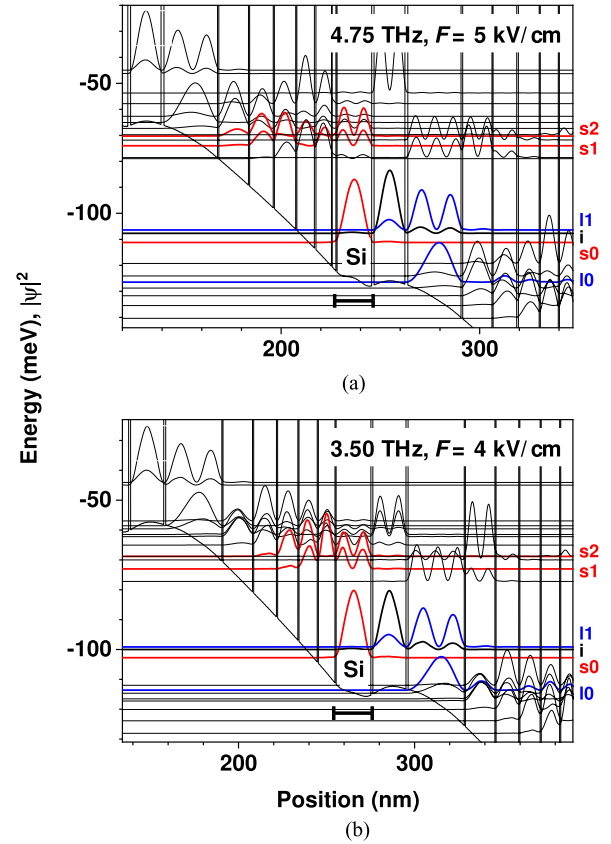


Fig. 1. Conduction band profiles, subband structures, and positions of the Si doping of QCLs for (a) 4.75 and (b) 3.50 THz. The blue lines depict the laser states (l1, l0), while the red lines indicate the initial (s1, s2) and final states (s0) for the main transitions, which are resonant to the energy of the longitudinal optical phonon. The thick black line presents the injector state (i). Note that the dipole matrix elements D_{l1-l0} for the lasing transition may vary with increasing field strengths as the coupling of the lower laser level to the quasi-miniband varies while the energy separation E_{l1-l0} is rather constant due to the vertical character of the transition. In order to evaluate the designs, gain spectra have to be calculated for a larger field strength range, as shown in [7]. For the given field strengths, the key design parameters are $E_{l1-l0} = 20.1 \text{ meV}$, $D_{l1-l0} = 4.1 \text{ nm}$, $E_{l1-i} = 1.4 \text{ meV}$, $E_{s2-s0} = 40.9 \text{ meV}$, $E_{s1-s0} = 37.2 \text{ meV}$ with a quasi-miniband width of 21.1 meV and $E_{l1-l0} = 14.5 \text{ meV}$, $D_{l1-l0} = 1.7 \text{ nm}$, $E_{l1-i} = 0.9 \text{ meV}$, $E_{s2-s0} = 34.0 \text{ meV}$, $E_{s1-s0} = 29.7 \text{ meV}$ with a quasi-miniband width of 16.1 meV for (a) and (b), respectively.

between the doped quantum well and the quantum well, in which the lasing transitions takes place, as shown in Fig. 1. Due to the applied electric field, the positive space charge in the doped quantum well and the negative space charge in the undoped injector quantum well lead to the formation of a local dipole, i.e., to local electric-field domains [14], [15]. This local dipole is expected to stabilize the laser operation over a wider range of applied field strengths by supporting the self-adjustment of the states involved in the carrier injection into the upper laser level. The self-adjustment can be explained by a concurrent reduction of the electron population in the undoped injector quantum well, since a higher applied field strength results in a stronger coupling of injector and upper laser states. While the former process leads to a lowering of the energy of the injector state, it compensates for the latter one, resulting in an extended dynamic range. This allows for a reasonable intrinsic tuning

range of the laser modes even for designs with a vertical laser transition as shown recently [16].

The longer periods of such hybrid designs reduce the internal electrical field strengths and consequently the leakage currents. In addition, the undoped quantum well spatially separates the dopants from the energy states of the lasing transitions reducing parasitic impurity scattering. However, these rather complex structures together with the thin AlAs barriers are challenging to simulate as well as to grow. For the development of high-performance lasers, optimization procedures are necessary, which include both, simulated and empirical data, for a number of wafers with refined layer thicknesses. In particular, the background doping density [17], which is difficult to control over a longer growth campaign, may affect the effective carrier density and, hence, the formation of the local dipole. It may consequently lead to a small but significant rearrangement of the injector and laser states.

The GaAs/AlAs materials system exhibits very high barriers, which may lead to rather large interface roughness scattering. However, the influence of this scattering process on the laser transition can be neglected, since the envelope wave functions of the laser states possess a rather small amplitude at the position of the barriers/interfaces in our design with a vertical laser transition as discussed in [7]. Due to interdiffusion, the interfaces between barriers and quantum wells show a grading rather than an abrupt transition. While the realistic band structure with graded interfaces is included in our design procedure [10], possible alloy scattering is again neglected since the alloy region is located at positions where the wave functions have a small amplitude.

III. GROWTH AND REALIZATION

The lasers were grown by molecular beam epitaxy, which is particularly challenging for the very thin AlAs barriers with 2–4 monolayer thicknesses. Our approach consists in nominal growth rates of 0.11 and 0.13 nm/s for AlAs and GaAs, respectively, leading to a minimum Al shutter opening time of 5 s for the thinnest barrier and an overall growth time of about 22 h for the whole cascade structure. The average growth rates amount to 0.13 nm/s, while fluctuations in the growth rates are below 1% due to the use of a closed-loop rate control system based on optical reflection measurements [18] for the *in-situ* growth control. During growth, the substrate was rotated at a speed of about 12 r/min, which is adjusted for each QCL structure so that it corresponds to an integer number of rotations per period of the cascade structure. For the waveguides, we followed [2] with reduced thicknesses of both, the top (80 nm) and bottom (700 nm), GaAs layers. The samples were processed by photolithography and standard wet chemical etching for the (Al,Ga)As materials system using an identical procedure for all lasers. The etching solution is $\text{H}_2\text{SO}_4:\text{H}_2\text{O}_2:\text{H}_2\text{O}$ (1:1:8). The metal contacts were made from $\text{Ni}/\text{Au}_{0.995}\text{Ge}_{0.005}$ (10/150 nm) and annealed at 450 °C in order to achieve Ohmic contacts.

The lasers are operated in a helium flow cryostat (Oxford Optistat CF-V), a Stirling cryocooler (Ricor K535), as shown in Fig. 2(a), or in a miniature Stirling cryocooler (AIM SL400),

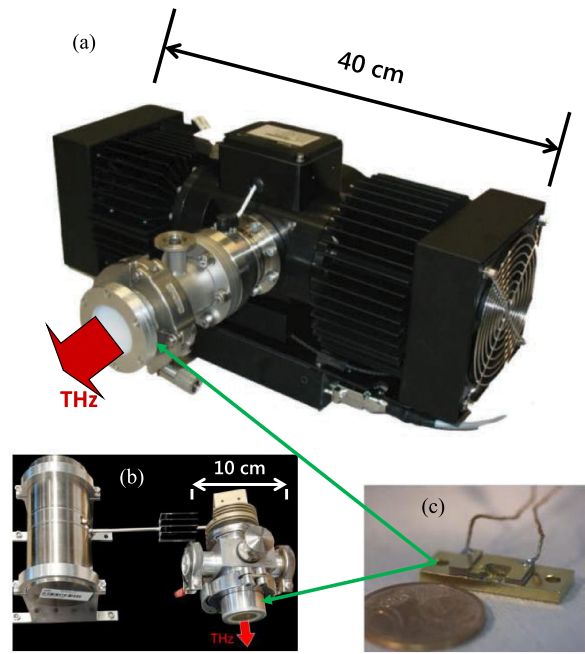


Fig. 2. Photographs of (a) the Stirling cryocooler, (b) the miniature Stirling cryocooler consisting of a cold finger mounted in a vacuum housing and a cylindrical compressor unit, and (c) the QCL on a copper submount. The THz beams, indicated by the red arrows, pass the vacuum housings through an exit window made of either polyethylene, poly-4-methylpentene-1 (TPX), or polypropylene.

as shown in Fig. 2(b). The miniature cryocooler consists of two components, a cold finger mounted in a vacuum housing and a cylindrical compressor unit. The gold-plated copper submounts with the QCLs shown in Fig. 2(c) are mounted to the respective cold finger of the used cooler. The lasing spectra are measured using a Fourier-transform infrared spectrometer Bruker Vertex 80v, while the output power was determined using a calibrated power meter (Laserprobe RkP-575 RF).²

IV. RESULTS

Fig. 3 exhibits a compilation of operating parameters of 21 GaAs/AlAs QCLs. For 3.50 and 4.75 THz, three different wafers were used, while for 3.92 THz the lasers were fabricated from two different wafers. For all other frequencies, only one wafer was used to fabricate lasers. All QCLs are based on the hybrid active-region design. The output power of Fabry-Pérot lasers based on single-plasmon waveguides is shown for cw operation as a function of the emission frequency. The typical ridge dimensions of these lasers are about $0.12 \times 1.0 \text{ mm}^2$, and their threshold current densities vary between 100 and 300 A/cm². For 3.50 and 4.75 THz, the optimization of the lasers has already started, which can be seen by the comparatively larger powers for these frequencies. The wall-plug efficiencies for lasers at 3.50 and 4.75 THz reach values larger than 1.8 and 1.1×10^{-3} , respectively, i.e., for typical output powers of 1 mW, electrical

²Power values are not corrected for window transmission losses or collection efficiency and are a lower bound by a factor of about 2 to the absolute power of the lasers.

TABLE I
LASER PARAMETERS FOR CONTINUOUS-WAVE OPERATION

QCL	ν_{\max} (THz)	ν_{mode} (THz)	T_{po} (K)	$\Delta\nu$ (GHz)	L (mW)	J_{th} (A/cm ²)	J_{\max} (A/cm ²)
A	3.5	3.41 – 3.50	65	5	4.7	240	490
B	4.1	3.94 – 3.98	50	11	1.6	190	460
C	4.8	4.67 – 4.80	55	7	4.4	220	510

ν_{\max} denotes the frequency of the calculated gain maximum, ν_{mode} the frequency range of the observed lasing modes, T_{po} the practical operating temperature, $\Delta\nu$ the intrinsic tuning range, L the output power, J_{th} the threshold current density, and J_{\max} the current density at the maximum of the output power. The values for $\Delta\nu$, L , J_{th} , and J_{\max} have been determined for a heat-sink temperature of 30 K.

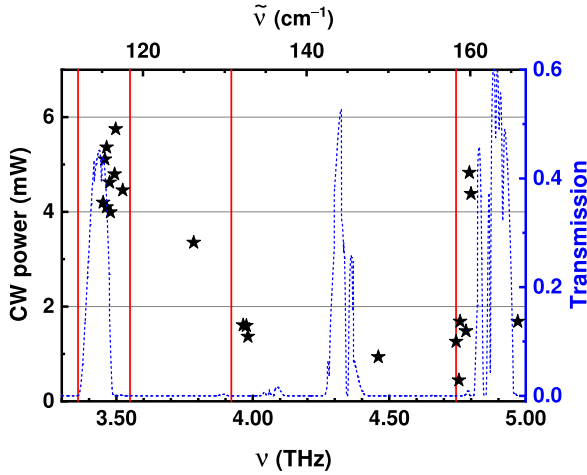


Fig. 3. Maximum output power for cw operation as a function of the center emission frequency for 21 GaAs/AlAs QCLs (asterisks) based on the hybrid active-region design measured at a heat sink temperature of 30 K. The vertical lines indicate the target frequencies of 3.36, 3.92, and 4.75 THz for fine-structure transitions of Al, N⁺, and O atoms/ions, respectively, and 3.55 THz for OH detection. The dashed line depicts a simulated transmission spectrum of air based on the HITRAN database³ for ambient conditions corresponding to the USA model, mean latitude, summer, and an optical path length of 10 m, exhibiting maxima at 3.43, 4.32, and 4.92 THz.

powers of less than 1 W are required so that the operation in a miniature cryocooler becomes feasible.

We will now present the operating parameters for exemplary lasers emitting at frequencies around 3.50, 3.90, and 4.75 THz in more detail. Table I summarizes the frequencies of the calculated gain maxima, the frequency ranges of the observed laser modes, and the practical operating temperature, as well as for 30 K the intrinsic tuning ranges, the output powers, the threshold current densities, and the current densities at the maxima of output power for QCLs A, B, and C. Fig. 4 shows the light output-current density-voltage (L - J - V) characteristics as well as the lasing spectra of QCL A⁴ with emission frequencies between 3.40 and 3.50 THz observed for various operating conditions. At 30 K, the threshold current density is as low as 240 A/cm², although the confinement factor in the employed single-plasmon waveguide

³hitran.iao.ru

⁴QCL A has been fabricated from wafer PDI-M4-3322. Starting from the injection barrier, indicating AlAs and GaAs layers by bold and normal font, respectively, and denoting the Si-doped quantum well ($n_{\text{Si}} = 2.0 \times 10^{17} \text{ cm}^{-3}$) by underlining its thickness, the nominal thicknesses of the layers in nm are: **0.84**/32.2/0.48/16.9/**0.48**/13.1/**0.48**/11.7/**0.48**/10.5/0.48/9.6/**0.48**/20.0/**0.84**/19.1. The quantum well doping corresponds to an average doping of $2.9 \times 10^{16} \text{ cm}^{-3}$ and a sheet carrier density of $4.0 \times 10^{11} \text{ cm}^{-2}$ per period.

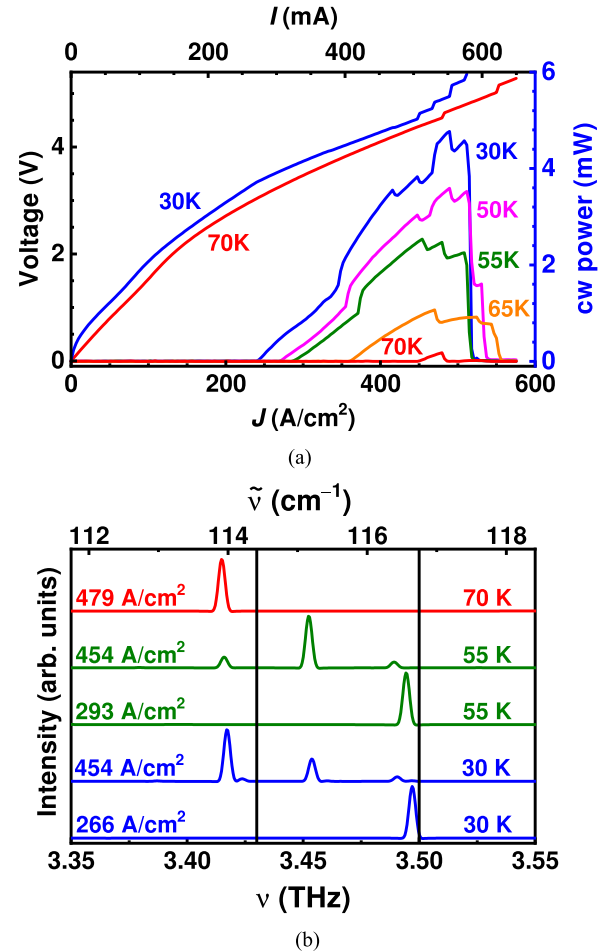


Fig. 4. (a) L - J - V characteristics for several operating temperatures and (b) lasing spectra for several operating temperatures and current densities of QCL A with laser ridge dimensions of $0.12 \times 0.94 \text{ mm}^2$ under cw operation. The vertical solid lines indicate the target frequencies of 3.43 and 3.50 THz.

is rather low (about 0.5). The tuning range for individual lasing modes amounts to about 5 GHz, which is sufficient for high-resolution spectroscopy of low-pressure molecular absorption lines, for example, of methanol. Applying first-order distributed-feedback gratings [19], [20] or two-section cavities [21], [22], this wafer can be used for the fabrication of single-mode lasers operating around 3.50 THz for the detection of OH. The value for T_{po} is currently 65 K, which can be improved by varying the shape of the ridge laser. The target frequency of 3.36 THz for the respective fine-structure transition of Al atoms can be reached by a minor adjustment of the active region.

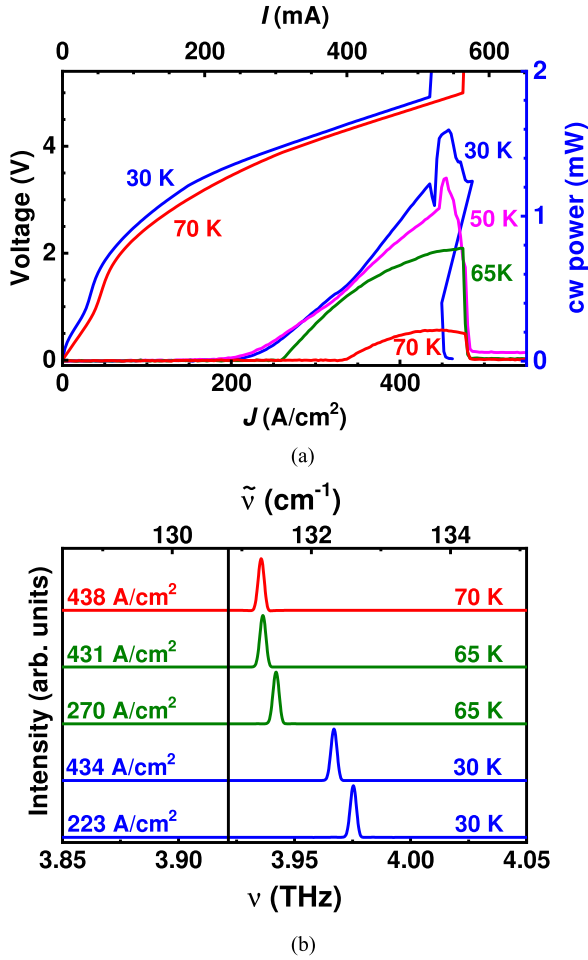


Fig. 5. (a) L - J - V characteristics for several operating temperatures and (b) lasing spectra for several operating temperatures and current densities of QCL B with laser ridge dimensions of 0.12×0.99 mm² under cw operation. The vertical solid line indicates the target frequency of 3.92 THz.

The L - J - V characteristics as well as the lasing spectra of the least optimized QCL B,⁵ which emits at about 3.90 THz, are shown in Fig. 5. The output power is lower than for QCL A, although it may be sufficient for high-resolution absorption spectroscopy of the fine-structure transition of N⁺ ions. The tuning range at 30 K is about 11 GHz, which is rather large.

Fig. 6 displays the L - J - V characteristics as well as the lasing spectra of QCL C,⁶ which emits at 4.745 THz. It is the most

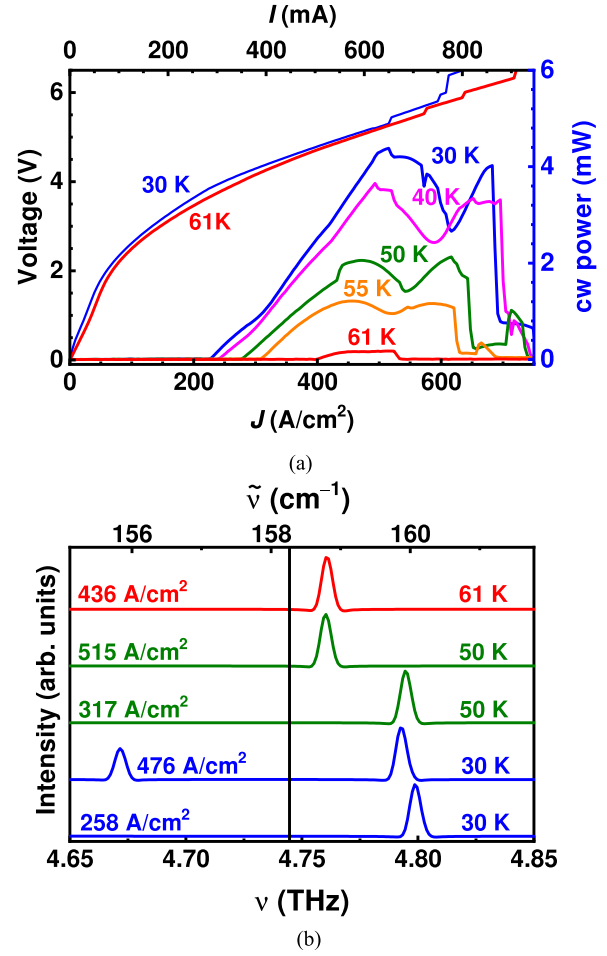


Fig. 6. (a) L - J - V characteristics for several operating temperatures and (b) lasing spectra for several operating temperatures and current densities of QCL C with laser ridge dimensions of 0.12×1.05 mm² under cw operation. The vertical solid line indicates the target frequency of 4.745 THz.

⁵QCL B has been fabricated from wafer PDI-M4-3417. Starting from the injection barrier, indicating AlAs and GaAs layers by bold and normal font, respectively, and denoting the Si-doped quantum well ($n_{\text{Si}} = 1.5 \times 10^{17}$ cm⁻³) by underlining its thickness, the nominal thicknesses of the layers in nm are: **1.12/29.9/0.56/16.1/0.42/12.8/0.42/11.3/0.42/9.6/0.42/8.8/0.42/19.1/0.84/19.1**. The quantum well doping corresponds to an average doping of 2.2×10^{16} cm⁻³ and a sheet carrier density of 2.9×10^{11} cm⁻² per period.

⁶QCL C has been fabricated from wafer PDI-M4-3148. Starting from the injection barrier, indicating AlAs and GaAs layers by bold and normal font, respectively, and denoting the Si-doped quantum well ($n_{\text{Si}} = 2.0 \times 10^{17}$ cm⁻³) by underlining its thickness, the nominal thicknesses of the layers in nm are: **1.12/27.2/0.56/15.0/0.42/12.1/0.42/10.8/0.42/9.2/0.42/8.1/0.28/2.0/0.28/17.7/1.12/15.7**. The quantum well doping corresponds to an average doping of 2.9×10^{16} cm⁻³ and a sheet carrier density of 3.5×10^{11} cm⁻² per period.

mature QCL out of this series. Even for this comparatively large emission frequency, an output power of about 4 mW is achieved at 30 K, when the laser is operated in a helium-flow cryostat for laser ridge dimensions of 0.12×1.05 mm². The gain maximum is close to the target frequency. Based on this design, we fabricated lasers with an improved output power using ridge dimensions of 0.08×0.90 and 0.08×0.87 mm². Operated in a mechanical cryocooler, we demonstrated $T_{\text{po}} > 70$ K, as shown in Fig. 7(a). These lasers can readily be operated in a miniature cryocooler with a cooling power of about 1 W. Fig. 7(b) shows the beam profile obtained by using a TPX lens in this configuration. Using enhanced back-facet reflection, another laser out of this series operated in the miniature cryocooler has recently been shown to provide up to 8 mW output power. This QCL emits a single mode around the rest frequency of atomic oxygen, which can be tuned from -2.7 to $+9.4$ GHz [23]. A similar laser has been tested in a spectrometer to be used for plasma diagnostics. Fig. 8 shows an absorption line of NH₃ at 4.767 THz. Static fine-tuning of this laser to 4.745 THz following the procedure described by B. Röben *et al.* [24] is finally expected to allow for the detection of atomic oxygen in the plasma reactor.

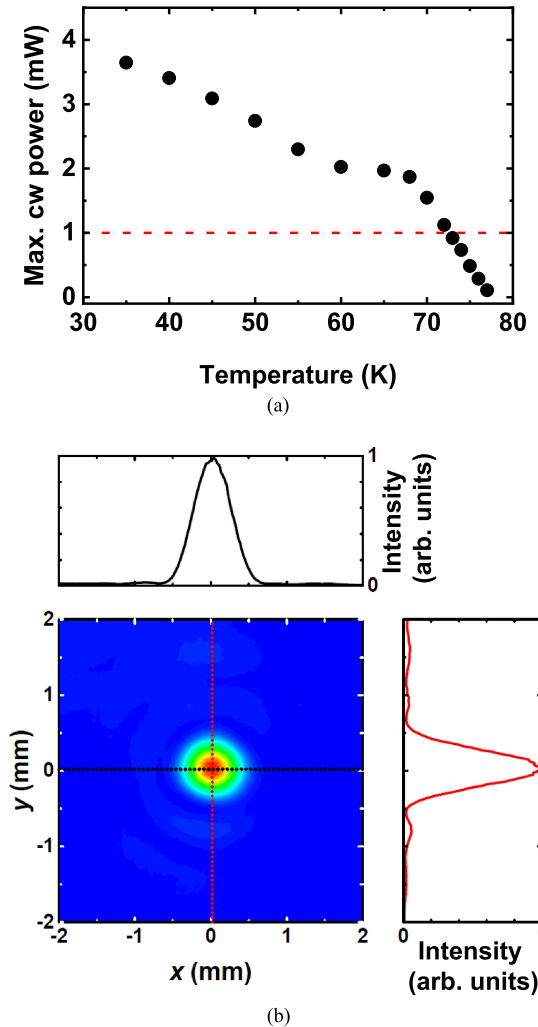


Fig. 7. (a) Maximum output power under cw operation as a function of heat-sink temperature for a laser with ridge dimensions of $0.08 \times 0.87 \text{ mm}^2$ emitting at 4.75 THz operated in a Stirling cooler. The dashed line indicates the power of 1 mW as a guide to the eye. (b) Beam profile of the 4.75-THz QCL (ridge dimensions $0.08 \times 0.90 \text{ mm}^2$) operated in a miniature Stirling cryocooler.

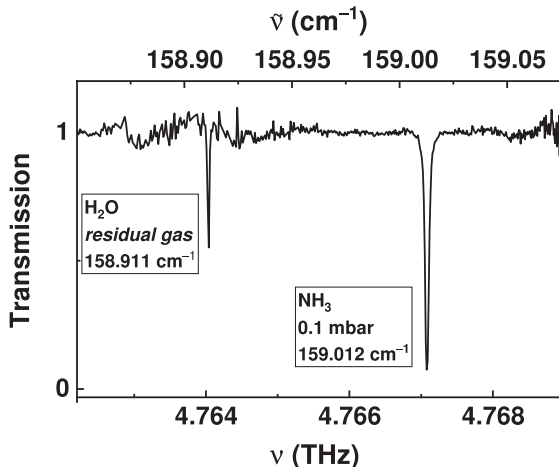


Fig. 8. Absorption spectrum of NH_3 around 4.767 THz using QCL C and a 15-cm-long absorption cell.

V. CONCLUSION

We have shown that THz QCLs based on GaAs/AlAs heterostructures can be designed for emission at various frequencies between 3.4 and 5.0 THz with output powers of several mW using single-plasmon waveguides. We expect that QCLs emitting at any frequency in the range between 3.4 and 5.0 THz can be developed by a straightforward interpolation of the presented designs. In particular, QCLs emitting at the target frequencies indicated in Fig. 3 can be realized by relying on the basic design in the GaAs/AlAs materials system. By optimizing the balance between the electric-field-dependent gain spectra and the non-linear transport properties, i.e., the onset of negative differential conductance, the operating parameters such as the output power and T_{po} may be further improved. The straightforward design of the resonators allows for a similarly straightforward fine-tuning of the laser modes so that these lasers are suitable for several practical applications in the field of high-resolution THz spectroscopy. The improved wall-plug efficiencies of GaAs/AlAs THz QCLs make them suitable for spaceborne applications, where a high T_{po} is required, in particular for passive cooling.

ACKNOWLEDGMENT

The authors would like to thank W. Anders, M. Hörnicke, A. Riedel, and A. Tahraoui for sample preparation, U. Macherius and F. Weichbrodt for technical assistance with the spectroscopic setup, as well as T. Flissikowski for a careful reading of the article. The view expressed in this article can in no way be taken to reflect the official opinion of the European Space Agency.

REFERENCES

- [1] J. Faist *et al.*, “Quantum cascade laser,” *Science*, vol. 264, pp. 553–556, Apr. 1994, doi: [10.1126/science.264.5158.553](https://doi.org/10.1126/science.264.5158.553).
- [2] R. Köhler *et al.*, “Terahertz semiconductor-heterostructure laser,” *Nature*, vol. 417, pp. 156–159, May 2002, doi: [10.1038/417156a](https://doi.org/10.1038/417156a).
- [3] J. R. Gao *et al.*, “Terahertz heterodyne receiver based on a quantum cascade laser and a superconducting bolometer,” *Appl. Phys. Lett.*, vol. 86, Jun. 2005, Art. no. 244104, doi: [10.1063/1.1949724](https://doi.org/10.1063/1.1949724).
- [4] H.-W. Hübers *et al.*, “Terahertz quantum cascade laser as local oscillator in a heterodyne receiver,” *Opt. Express*, vol. 13, no. 15, pp. 5890–5896, Jul. 2005, doi: [10.1364/OPEX.13.005890](https://doi.org/10.1364/OPEX.13.005890).
- [5] L. Schrottke *et al.*, “Quantum-cascade lasers as local oscillators for heterodyne spectrometers in the spectral range around 4.745 THz,” *Semicond. Sci. Technol.*, vol. 28, Feb. 2013, Art. no. 035011, doi: [10.1088/0268-1242/28/3/035011](https://doi.org/10.1088/0268-1242/28/3/035011).
- [6] H. Richter *et al.*, “4.7-THz local oscillator for the GREAT heterodyne spectrometer on SOFIA,” *IEEE Trans. THz Sci. Technol.*, vol. 5, no. 4, pp. 539–545, Jul. 2015.
- [7] L. Schrottke, X. Lü, G. Rozas, K. Biermann, and H. T. Grahn, “Terahertz GaAs/AlAs quantum-cascade lasers,” *Appl. Phys. Lett.*, vol. 108, Mar. 2016, Art. no. 102102, doi: [10.1063/1.4943657](https://doi.org/10.1063/1.4943657).
- [8] B. S. Williams, S. Kumar, H. Callebaut, Q. Hu, and J. L. Reno, “Terahertz quantum-cascade laser at $\lambda \approx 100 \mu\text{m}$ using metal waveguide for mode confinement,” *Appl. Phys. Lett.*, vol. 83, no. 11, pp. 2124–2126, Sep. 2003, doi: [10.1063/1.1611642](https://doi.org/10.1063/1.1611642).
- [9] B. S. Williams, “Terahertz quantum-cascade lasers,” *Nature Photon.*, vol. 1, pp. 517–525, Sep. 2007, doi: [10.1038/nphoton.2007.166](https://doi.org/10.1038/nphoton.2007.166).
- [10] X. Lü, E. Luna, L. Schrottke, K. Biermann, and H. T. Grahn, “Determination of the interface parameter in terahertz quantum-cascade laser structures based on transmission electron microscopy,” *Appl. Phys. Lett.*, vol. 113, Oct. 2018, Art. no. 172101, doi: [10.1063/1.5042326](https://doi.org/10.1063/1.5042326).
- [11] R. Köhler *et al.*, “Terahertz quantum-cascade lasers based on an interlaced photon-phonon cascade,” *Appl. Phys. Lett.*, vol. 84, no. 8, pp. 1266–1268, Feb. 2004, doi: [10.1063/1.1650905](https://doi.org/10.1063/1.1650905).

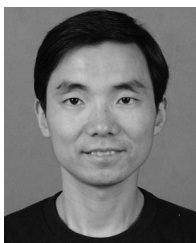
- [12] G. Scalari, N. Hoyler, M. Giovannini, and J. Faist, "Terahertz bound-to-continuum quantum-cascade lasers based on optical-phonon scattering extraction," *Appl. Phys. Lett.*, vol. 86, Apr. 2005, Art. no. 181101, doi: [10.1063/1.1920407](https://doi.org/10.1063/1.1920407).
- [13] M. I. Amanti *et al.*, "Bound-to-continuum terahertz quantum cascade laser with a single-quantum-well phonon extraction/injection stage," *New J. Phys.*, vol. 11, Dec. 2009, Art. no. 125022, doi: [10.1088/1367-2630/11/12/125022](https://doi.org/10.1088/1367-2630/11/12/125022).
- [14] V. D. Jovanović *et al.*, "Mechanisms of dynamic range limitations in GaAs/AlGaAs quantum-cascade lasers: Influence of injector doping," *Appl. Phys. Lett.*, vol. 86, May 2005, Art. no. 211117, doi: [10.1063/1.1937993](https://doi.org/10.1063/1.1937993).
- [15] S. L. Lu, L. Schrottke, S. W. Teitworth, R. Hey, and H. T. Grahn, "Formation of electric-field domains in GaAs/Al_xGa_{1-x}As quantum cascade laser structures," *Phys. Rev. B*, vol. 73, Jan. 2006, Art. no. 033311, doi: [10.1103/PhysRevB.73.033311](https://doi.org/10.1103/PhysRevB.73.033311).
- [16] L. Schrottke *et al.*, "Intrinsic frequency tuning of terahertz quantum-cascade lasers," *J. Appl. Phys.* vol. 123, May 2018, Art. no. 213102, doi: [10.1063/1.524480](https://doi.org/10.1063/1.524480).
- [17] L. H. Li, J. X. Zhu, L. Chen, A. G. Davies, and E. H. Linfield, "The MBE growth and optimization of high performance terahertz frequency quantum cascade lasers," *Opt. Express*, vol. 23, no. 3, pp. 2720–2729, Jan. 2015, doi: [10.1364/OE.23.002720](https://doi.org/10.1364/OE.23.002720).
- [18] A. W. Jackson, P. R. Pinsukanjana, A. C. Gossard, and L. A. Coldren, "In situ monitoring and control for MBE growth of optoelectronic devices," *IEEE J. Sel. Topics Quantum Electron.*, vol. 3, no. 3, pp. 836–844, Jun. 1997.
- [19] M. I. Amanti, G. Scalari, F. Castellano, M. Beck, and J. Faist, "Low divergence Terahertz photonic-wire laser," *Opt. Express*, vol. 18, no. 6, pp. 6390–6395, Mar. 2010, doi: [10.1364/OE.18.006390](https://doi.org/10.1364/OE.18.006390).
- [20] M. Wienold *et al.*, "Lateral distributed-feedback gratings for single-mode, high-power terahertz quantum-cascade lasers," *Opt. Express*, vol. 20, no. 10, pp. 11207–11217, May 2012, doi: [10.1364/OE.20.011207](https://doi.org/10.1364/OE.20.011207).
- [21] H. Li *et al.*, "Coupled-cavity terahertz quantum cascade lasers for single mode operation," *Appl. Phys. Lett.*, vol. 104, Jun. 2014, Art. no. 241102, doi: [10.1063/1.4884056](https://doi.org/10.1063/1.4884056).
- [22] M. Hempel *et al.*, "Continuous tuning of two-section, single-mode terahertz quantum-cascade lasers by fiber-coupled, near-infrared illumination," *AIP Adv.*, vol. 7, May 2017, Art. no. 055201, doi: [10.1063/1.4983030](https://doi.org/10.1063/1.4983030).
- [23] T. Hagelschuer *et al.*, "A compact 4.75-THz source based on a quantum-cascade laser with a back-facet mirror," *IEEE Trans. THz Sci. Technol.*, vol. 9, no. 6, pp. 606–612, Nov. 2019.
- [24] B. Röben, X. Lü, K. Biermann, L. Schrottke, and H. T. Grahn, "Terahertz quantum-cascade lasers for high-resolution spectroscopy of sharp absorption lines," *J. Appl. Phys.*, vol. 125, Apr. 2019, Art. no. 151613, doi: [10.1063/1.5079701](https://doi.org/10.1063/1.5079701).



Lutz Schrottke received the Diplom and doctoral degree in experimental physics from the Humboldt-Universität zu Berlin, Berlin, Germany, in 1983 and 1988, respectively.

From 1985 to 1991, he was with the Zentralinstitut für Elektronenphysik, Berlin, Germany, working on thin-film electroluminescent devices. In 1992, he joined the Paul-Drude-Institut für Festkörperelektronik, Berlin, Germany, as a scientific staff member. He was a Visiting Scholar with the Department of Physics, the University of Michigan, Ann Arbor,

MI, USA, from 1995 to 1996. His research interests include THz quantum-cascade lasers as well as optical and transport properties of semiconductor heterostructures.



Xiang Lü received the M.Sc. degree in physics from Soochow University, Suzhou, China, in 2000, and the Ph.D. degree in physics from the Shanghai Institute for Technical Physics, Chinese Academy of Sciences, Shanghai, China, in 2003.

He is currently a Postdoctoral Research Assistant with the Paul-Drude-Institut für Festkörperelektronik, Berlin, Germany, where he is involved in the field of THz quantum-cascade lasers.



Benjamin Röben studied physics with the Technische Universität Berlin, Berlin, Germany, and with Université Joseph Fourier, Grenoble, France. He received the M.Sc. and doctoral degrees from the Technische Universität Berlin, in 2014 and 2018, respectively.

He is currently a Postdoctoral Researcher with the Paul-Drude-Institut für Festkörperelektronik, Berlin, Germany focusing on the development of terahertz quantum-cascade lasers for spectroscopic applications.



Klaus Biermann received the Diplom in physics from the Friedrich-Alexander Universität, Erlangen-Nürnberg, Germany, in 1998, and the doctoral degree in physics from the Humboldt-Universität zu Berlin, Berlin, Germany, in 2007.

From 1998 to 2007, he was a Scientist with the Heinrich-Hertz-Institut für Nachrichtentechnik and the Max-Born-Institut für Nichtlineare Optik und Kurzzeitspektroskopie, both in Berlin, Germany, on molecular beam epitaxy (MBE) and femto-second spectroscopy of III–V semiconductor heterostructures with sub-ps response times, respectively. In 2007, he joined the Paul-Drude-Institut für Festkörperelektronik, Berlin, Germany, working on MBE of GaAs-based structures, focusing on the growth on substrates of various crystal orientations, overgrowth of patterned templates, and closed-loop *in-situ* control methods.

From 1998 to 2007, he was a Scientist with the Heinrich-Hertz-Institut für Nachrichtentechnik and the Max-Born-Institut für Nichtlineare Optik und Kurzzeitspektroskopie, both in Berlin, Germany, on molecular beam epitaxy (MBE) and femto-second spectroscopy of III–V semiconductor heterostructures with sub-ps response times, respectively. In 2007, he joined the Paul-Drude-Institut für Festkörperelektronik, Berlin, Germany, working on MBE of GaAs-based structures, focusing on the growth on substrates of various crystal orientations, overgrowth of patterned templates, and closed-loop *in-situ* control methods.



Till Hagelschuer received the M.Sc. degree in physics from Freie Universität, Berlin, Germany, in 2014, and the Ph.D. degree in physics from the Humboldt-Universität zu Berlin, Berlin, Germany, in 2018.

He is currently a Postdoctoral Researcher with the DLR's Institute of Optical Sensor Systems, Berlin, Germany. His research involves the application of external optical feedback phenomena in THz quantum-cascade lasers for high-resolution spectroscopy and imaging.

Dr. Hagelschuer was awarded for an outstanding student paper by the International Society of Infrared, Millimeter, and Terahertz Waves, in 2017.



Martin Wienold received the Diplom and doctoral degree in physics from the Humboldt-Universität zu Berlin, Berlin, Germany, in 2007 and 2012, respectively, working on mid-infrared and THz quantum-cascade lasers.

He is currently a Postdoctoral Research Assistant with the German Aerospace Center, Berlin, Germany, working on the development of spectroscopic techniques based on THz quantum-cascade lasers.



Heinz-Wilhelm Hübers received the Diplom and doctoral degree in physics from the Universität Bonn, Bonn, Germany, in 1991 and 1994, respectively.

From 1991 to 1994, he was with the Max-Planck-Institut für Radioastronomie, Bonn, Germany. In 1994, he joined the Deutsches Zentrum für Luft- und Raumfahrt (German Aerospace Center, DLR), Berlin, Germany, becoming the Head of Department in 2001. From 2009 to 2014, he has been a Professor of experimental physics with the Technische Universität Berlin, Berlin, Germany, and the Head of the

Department “Experimental Planetary Physics” at DLR. In 2014, he became the Director of the Institute of Optical Sensor Systems, DLR and a Professor with the Humboldt-Universität zu Berlin. His research interests include THz physics and spectroscopy, particularly in THz systems for astronomy, planetary research, and security.

Prof. Hübers has received the Innovation Award on Synchrotron Radiation (2003) and the Lilienthal Award (2007).



Mario Hannemann received the Diplom and doctoral degree in experimental physics from the Ernst-Moritz-Armdt-Universität (EMAU) Greifswald, Greifswald, Germany, in 1980 and 1992, respectively.

From 1980 to 1985, he was a Research Assistant with EMAU, working on plasma diagnostics. From 1985 to 1991, he was with the Zentralinstitut für Elektronenphysik, Berlin, Germany, working on photometric evaluation and optimization of high-pressure light sources as well as calculation of

material functions of high-pressure lamp plasmas. In 1992, he joined the Institut für Niedertemperatur-Plasmaphysik, later Leibnizinstitut für Plasmaforschung und Technologie, Greifswald, Germany, as a scientific staff member, working again in the field of plasma diagnostics, especially on Langmuir probe diagnostics and laser absorption spectroscopy.



Jean-Pierre H. van Helden received the M.Sc. and Ph.D. degrees in applied physics from the Eindhoven University of Technology, Eindhoven, The Netherlands, in 2001 and 2006, respectively.

From 2007 to 2012, he was a Postdoctoral Research Assistant with the Department of Chemistry, the University of Oxford, working on laser spectroscopy of molecular gases and plasmas. In 2012, he joined the Leibniz Institute for Plasma Science and Technology (INP), Greifswald, Germany, working on laser-based plasma diagnostics. In 2017, he was appointed the

Head of the Department of Plasma Diagnostics, INP. His main research interests include the kinetics and chemistry of low and atmospheric pressure plasmas and laser spectroscopy with a particular focus on the development of diagnostics to characterize plasmas and their interactions with surfaces. Since a few years, the focus has been on cavity-enhanced laser-based diagnostics for plasmas using lasers in the mid- and far-infrared and frequency comb spectroscopy.



Jürgen Röpcke received the Diplom and Ph.D. degree in experimental physics from Ernst-Moritz-Armdt-Universität (EMAU) Greifswald, Greifswald, Germany, in 1981 and 1987, respectively, followed by the habilitation in 2002.

From 1981 to 1982, he was a Research Assistant with EMAU, working in the field of laser metrology. From 1982 to 1991, he was with the Central Institute of Electron Physics, Academy of Science, Greifswald, Germany, studying discharge processes in plasma displays. In 1992, he joined the Leibniz Institute for Plasma Science and Technology (INP), Greifswald, Germany, working

on spectroscopic plasma diagnostics. In 2005, he was appointed as a Professor for plasma technique with the University of Applied Science Stralsund. His scientific interests are focused on the investigation of kinetics and chemistry of molecular nonisothermal plasmas based on state-of-the-art optical diagnostics.



Holger T. Grahn received the Diplom in physics from the Universität Kiel, Kiel, Germany, in 1983, and the Ph. D. degree in physics from Brown University, Providence, RI, USA, in 1987.

From 1988 to 1992, he was a Postdoctoral Research Assistant with the Max-Planck-Institut für Festkörperforschung, Stuttgart, Germany, working on vertical transport in semiconductor superlattices. In 1992, he joined the Paul-Drude-Institut für Festkörperelektronik, Berlin, Germany, as a Department Head, first for Analytics and later for Semiconductor

Spectroscopy. In 2001, he was appointed an Adjunct Professor in physics with the Technische Universität Berlin, Berlin, Germany. His research interests include the optical and transport properties of semiconductor heterostructures and THz quantum-cascade lasers.